

RESEARCH

Open Access



MiRNA-mRNA network in osteoporotic fractures proposes the functional mechanism of hsa-miR-32-3p/TNFSF11 axis

Yukai Zeng^{1,6†}, Bo Zhao^{2†}, Jiawei Gong³, Qingfeng Zhang⁴ and Fei Yang^{5*}

Abstract

Background and aims This study aimed to construct a miRNA-mRNA network in OF and explored the effect of the hsa-miR-32-3p/TNFSF11 axis on osteoclast function.

Methods GSE70318 and GSE74209 datasets were used to filter the differentially expressed miRNAs in OF. Then, the targets of these miRNAs intersected with the disease genes of OF. The target genes were annotated using GO terms and KEGG pathway enrichment analysis. The network for miRNA-gene-top 30 GO terms/top 20 pathways was drawn. Sankey diagrams were drawn for Parathyroid hormone synthesis, secretion, and action pathway (hsa04928) and ossification (GO:0001503) related to osteoporotic fracture. The hsa-miR-32-3p/TNFSF11 axis was selected for expression and functional verification.

Results A total of 21 differentially expressed miRNAs in OF were obtained by analyzing GSE70318 and GSE74209 datasets. A total of 36 genes were related to OF among the miRNA-targets. The genes were enriched in GO terms and KEGG pathways related to OF. Parathyroid hormone synthesis, secretion, and action pathway (hsa04928) and ossification proposed that the hsa-miR-32-3p/TNFSF11 axis may be involved in OF. The expression level of hsa-miR-32-3p was decreased in patients with low bone mineral density (BMD) and fracture, while the expression level of TNFSF11 mRNA was increased. Hsa-miR-32-3p complementarily bound with TNFSF11. Hsa-miR-32-3p inhibited osteoclast activation, while TNFSF11 promoted osteoclast activation.

Conclusions The miRNA-mRNA network in OF proposed the TNFSF11 as a downstream target of hsa-miR-32-3p. The hsa-miR-32-3p/TNFSF11 axis was involved in the regulation of osteoclast activity.

Clinical trial number Not applicable.

Keywords Osteoporotic fractures, Osteoclasts, MiRNA, TNFSF11, Hsa-miR-32-3p

[†]Yukai Zeng and Bo Zhao contributed equally to this work.

*Correspondence:

Fei Yang

feiyangdr1@163.com

¹School of Biomedical Engineering, Capital Medical University, Beijing 100069, China

²Department of Orthopedic 2, Zhongxian People's Hospital of Chongqing, Chongqing 404300, China

³Department of Spinal Surgery, Traditional Chinese Medicine Hospital of Kunshan, Suzhou 215300, China

⁴Spine Department, Beijing University of Chinese Medicine Third Affiliated Hospital, Beijing 100029, China

⁵Department of Orthopaedics, Zibo Central Hospital, No. 54, Gongqingtuan West Road, Zhangdian District, Zibo, Shandong 255036, China

⁶Department of Orthopedic Surgery, The Seventh Affiliated Hospital of Sun Yat-sen University, Shenzhen 518107, China



© The Author(s) 2025. **Open Access** This article is licensed under a Creative Commons Attribution-NonCommercial-NoDerivatives 4.0 International License, which permits any non-commercial use, sharing, distribution and reproduction in any medium or format, as long as you give appropriate credit to the original author(s) and the source, provide a link to the Creative Commons licence, and indicate if you modified the licensed material. You do not have permission under this licence to share adapted material derived from this article or parts of it. The images or other third party material in this article are included in the article's Creative Commons licence, unless indicated otherwise in a credit line to the material. If material is not included in the article's Creative Commons licence and your intended use is not permitted by statutory regulation or exceeds the permitted use, you will need to obtain permission directly from the copyright holder. To view a copy of this licence, visit <http://creativecommons.org/licenses/by-nc-nd/4.0/>.

Introduction

Osteoporotic fracture (OF) is a usual consequence of osteoporosis, which is closely related to the overactivation of osteoclasts (OCs) in the body [1, 2]. Bone remodeling is tightly regulated by crosstalk between osteoblasts, which regulate bone formation, and osteoclasts, which regulate bone resorption [3]. Osteoclasts can secrete soluble factors that influence osteoblast formation and differentiation [4]. Osteoclasts are multinuclear bone-absorbing cells from the monocyte-macrophage lineage, which are essential for normal bone development and bone balance in the body [3]. As the main cell type in the human body responsible for bone resorption, osteoclasts have become an important target for the prevention and treatment of osteoporotic fractures [5]. Biochemical markers of bone turnover can be used to manage therapy monitoring in osteoporotic patients [6, 7]. Antiresorptive treatments are currently leading therapy for osteoporosis [8–11]. Despite advances in osteoporosis research, the optimal pharmacotherapeutic strategies for both managing and preventing osteoporotic fractures remain a subject of ongoing debate within the clinical community [12].

The osteoclast differentiation factor, receptor activator for nuclear factor-kappa B ligand (RANKL/TNFSF11), not only promotes the differentiation and fusion of osteoclast precursor cells, but also activates mature osteoclasts, and is considered to be the final step in osteoclast activation [13]. Cytokine RANKL is essential for the formation of osteoclasts during physiological and pathological bone resorption [14]. Osteoprotegerin (OPG), a soluble decoy receptor, competitively binds to RANKL, preventing its interaction with RANK, thus regulating osteoclastogenesis [15]. High concentrations of RANKL can promote the number and activity of osteoclasts [16]. The RANKL/RANK/OPG system play a pivotal role in osteoclast differentiation and function [17].

MicroRNAs (miRNAs) are highly conserved single-stranded small non-coding RNA molecules that can regulate more than 30% of genes in eukaryotes [18]. MiRNAs can specifically bind to the 3'-untranslated region (3'-UTR) of the target, inhibiting the expression of mRNA by interfering with the stability of mRNA and/or blocking protein translation [19]. One miRNA can target many mRNAs, while one mRNA can be targeted by a lot of miRNAs [20, 21]. The dual role of miRNAs in OF can be shown with some miRNAs promoting osteogenesis while others inhibit it, such as miR-21 (promoting osteoclastogenesis) and miR-24-1-5p (inhibiting osteoblastogenesis) [21–23]. By inhibiting the expression of ELF3, miR-206 can increase the activity of ALP and OCN in osteoarthritis models, promote the proliferation of osteoblasts, and inhibit their apoptosis [24]. MiR-150 can inhibit TNF- α -induced osteoblast apoptosis and promote

osteoblast differentiation and autophagy [25]. Therefore, the network based on the communications of miRNAs and mRNAs is important for OF.

This study aimed to identify OF-related miRNAs and their target genes, as well as to analyze the regulatory network they form in OF. Based on the miRNA-mRNA network, the hsa-miR-32-3p/TNFSF11 axis was verified for the expression levels in our patient cohort and the function in osteoclast ossification activity.

Materials and methods

GEO database search

Using the search term “osteoporotic fractures” in the GEO database, GSE70318 was a dataset analyzed miRNA profile in skeletal fractures in post-menopausal women, while GSE74209 identified osteoporosis-related dysregulated miRNAs. For the GSE74209 dataset, data from all cases (six fresh bone samples from healthy control and six fresh bone samples from osteoporotic cases) were analyzed using the online tool GEO2R to obtain differentially expressed miRNAs (the absolute value of Fold changes greater than 2 and $p < 0.05$). For the GSE70318 dataset, we meticulously selected the OF cases without type-2 diabetes ($n = 17$, serum samples), and matched healthy controls ($n = 17$, serum samples) (Supplementary Table 1), to obtain differentially expressed miRNAs using the limma method (the absolute value of Fold changes > 1 , $p < 0.05$). GSE70318 used a lower cutoff due to sample size.

Collection of MiRNA target genes and disease genes

MiRNA target genes were collected using the microT-CDS database. Disease genes were collected using the DISGENET database, using “osteoporosis with fracture-C0521170” term. The common genes were identified via an intersection analysis using a Venn diagram.

Gene annotation

The OECloud tools were used to perform GO (Gene Ontology) and KEGG (Kyoto Encyclopedia of Genes and Genomes) enrichment analysis (p value < 0.05).

Network construction

(1) Whole miRNA-gene-GO/KEGG network: The genes and miRNAs associated with the top 30 GO terms and the top 20 KEGG pathways were traced back, respectively; and the miRNA-gene-GO/KEGG network was drawn using Cytoscape version 3.7.1.

(2) OF-related miRNA-gene-GO/KEGG network: OF-related GO term ossification (GO:0001503) and Parathyroid hormone synthesis, secretion, and action pathway (hsa04928) were backtracked to find the corresponding genes and miRNAs. The Sankey diagrams were drawn.

Case collection

The study was performed in line with the principles of the Declaration of Helsinki. Approval was granted by the Ethics Committee of Zibo Central Hospital before the study began. The written informed consent has been obtained from the participants involved.

30 healthy people, 30 people with low bone mineral density (BMD) but no fractures, and 30 people with low BMD and fractures were collected (Table 1). Age, gender, body mass index, and diabetes mellitus status were matched among groups. All cases had not received any treatment related to bone mineral density.

Induction of osteoclasts

Human bone marrow stem cells (hBMSCs) were purchased from Takara (USA). The hBMSCs were resuspended in a-MEM complete medium (HyClone, USA). The suspension was adjusted to a cell density of 3×10^6 cells/mL and cultured in a culture dish containing 10 ng/ml macrophage colony-stimulating factor (M-CSF) for 24 h. Non-adherent cells (the osteoclast precursor cells) were collected. The density of seeded cells was adjusted to 10^5 /ml, and 30 ng/mL M-CSF was added for 9 days of culture.

Cell transfection

hBMSCs were seeded at a density of 15,000 cells/cm² in a-MEM complete medium (HyClone, USA). Then, transfection was performed using lipofectamine 3000 (ThermoFisher, USA). After transfection, cells were subjected to osteoclast induction or other procedures.

Osteoclast quantification

After culture, the coverslips carried cells were stained with tartrate-resistant acid phosphatase (TRAP) stain kit

(Nanjing Jiancheng, China), and then TRAP staining was used to analyze the number of osteoclast-like cells.

RT-qPCR assay

Total RNA in serum or cells was extracted using TRIzol (Invitrogen, USA). For complementary DNA production, total RNA was treated with the miScript® II RT kit (QIAGEN, Germany) or PrimeScript RT reagent kit (Takara, Japan) following the manufacturer's instructions. RT-qPCR analyses were performed using the miScript® SYBR Green PCR Kit (QIAGEN, Germany) or iTaq™ Universal SYBR Green Supermix (Bio-Rad, USA) on a CFX96™ Real-Time PCR Detection System (Bio-Rad, USA). Data were analyzed using $2^{-\Delta\Delta t}$.

Dual luciferase reporter

The wild-type or mutant plasmids containing TNFSF11-3'UTR were constructed (wt-TNFSF11 and mut-TNFSF11). Then, wt-TNFSF11 and mut-TNFSF11 were co-transfected with has-miR-32-3p mimic or mimic NC into hBMSCs by Lipofectamine-3000 (ThermoFisher, USA). The fluorescence intensity was measured using a Dual-Luciferase® Reporter Assay System (Promega, USA) on a GloMax® Discover Microplate Luminometer.

Biotin RNA pulldown assay

Streptavidin beads (Invitrogen, USA) were coated with the biotin-labeled antisense probes (3 µg). hBMSCs were lysed in lysis buffer and then co-incubated with probe-coated streptavidin beads at 4°C overnight. After complex elution, the pull-down has-miR-32-3p was determined by RT-qPCR assays. Biotin-labelled sense probe (3 µg) was sampled as a negative control.

Western blot analysis

Following transfection and induction, cells were washed and then lysed in 100 µl of Radioimmunoprecipitation assay buffer (Sigma-Aldrich, USA). The supernatants of cell lysates after centrifugation were collected for western blot analysis. After separation in 10% SDS-PAGE, lysate staining was transferred to polyvinylidene fluoride membranes (GE Healthcare Life Sciences, USA). After block, each membrane was incubated with the primary antibodies, including anti-cathepsin K antibody (Sigma-Aldrich, USA) and anti-Oscar antibody (Creative Diagnostics, USA) at 4°C overnight. Horseradish peroxidase-conjugated immunoglobulin G was used as a secondary antibody. An enhanced chemiluminescence detection system (Cobas 8000 e 801, Roche, Germany) was used to detect immunoreactive proteins.

Statistical analysis

Statistical differences between groups were analyzed by ordinary one-way analysis of variance (ANOVA); the

Table 1 The demographic characteristics of the patient cohort used for RT-qPCR analysis

Parameters	Healthy control (n=30)	Low-BMD without fractures (n=30)	Low BMD with fractures (n=30)	P value
Age (years)	33.9±13.5	35.3±11.8	37.5±12.8	0.670 ^a ; 0.497 ^b ; 0.297 ^c
Gender (male/female)	9/21	10/20	12/18	0.709
Body Mass Index	22.8±3.1	21.8±2.6	22.8±2.8	0.201 ^a ; 0.169 ^b ; 0.958 ^c
Diabetes mellitus	7	10	5	0.319

a, Low-BMD without fractures vs. Healthy control; b, Low BMD with fractures vs. Low-BMD without fractures; c, Low BMD with fractures vs. Healthy control

Comparison of age and Body Mass Index was conducted using Mann-Whitney U test; Comparison of gender and diabetes mellitus was conducted using Chi-square test

relationship between the expression levels of hsa-miR-32-3p and TNFSF11 was evaluated by Pearson's correlation; $p < 0.05$ was considered statistically significant.

Results

Differentially expressed miRNAs in OF

GSE70318 and GSE74209 datasets were used to screen miRNAs associated with OF (Fig. 1). Among them, the GSE70318 dataset obtained 35 miRNAs differentially expressed in OF (Fig. 2A); while GSE74209 dataset screened 156 differentially expressed miRNAs (Fig. 2B). After an intersection analysis using a Venn diagram, these two datasets obtained 21 common miRNAs (Fig. 2C).

Targets of differentially expressed miRNAs against OF

Through target gene prediction, the 21 miRNAs obtained from the GSE70318 and GSE74209 datasets can target 5614 target genes (Fig. 3A). After overlapping with OF-related genes from the DISGENET database, thirty-six of the miRNA-target genes were identified as OF-related genes (Fig. 3B). After GO enrichment analysis, these 36 target genes were found to be related to OF-related biological processes, such as ossification (Fig. 3C). After KEGG pathway enrichment analysis, it was found that these 36 target genes were enriched in multiple pathways, including OF-associated Parathyroid hormone synthesis, secretion, and action pathway (Fig. 3C). The top 30 GO terms and top 20 KEGG pathways were traced back to find genes and miRNAs, and then the miRNA-gene-GO/KEGG network was constructed (Fig. 4).

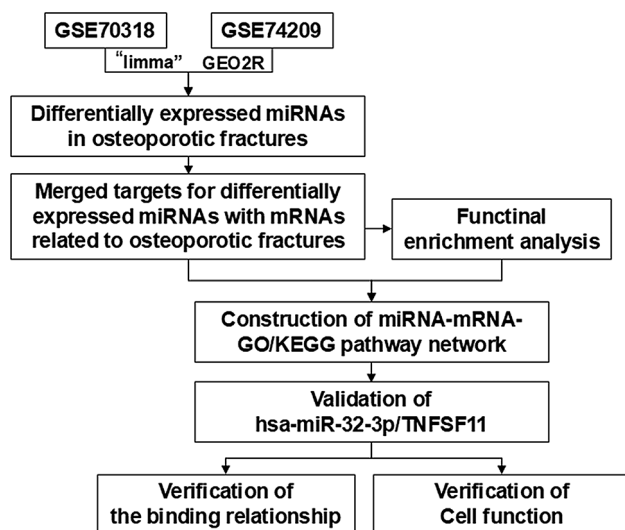


Fig. 1 The flowchart of this study

The expression levels of hsa-miR-32-3p and TNFSF11 in OF Endocrine regulators, including parathyroid hormone, participates in the bone remodelling cycle [26]. By tracing back to the Parathyroid hormone synthesis, secretion, and action pathway and the ossification biological process, we found that the axis composed of hsa-miR-32-3p and TNFSF11 can target these two OF-related items (Fig. 5A). Therefore, we selected this miRNA for the further investigation. Through RT-qPCR analysis, we found that the expression level of hsa-miR-32-3p in low BMD with fractures was lower than that in healthy controls and low BMD without fractures (Fig. 5B). The expression level of TNFSF11 mRNA in low BMD with fractures was higher than that in healthy controls and low BMD without fractures (Fig. 5C). Moreover, the expression levels of hsa-miR-32-3p and TNFSF11 were negatively correlated (Fig. 5D).

Verification of the binding relationship between hsa-miR-32-3p and TNFSF11

To verify the binding relationship between hsa-miR-32-3p and TNFSF11, we performed a dual luciferase reporter experiment using hBMSCs. The results showed that hsa-miR-32-3p mimic could reduce the fluorescence intensity of wild-type TNFSF11, but did not influence the fluorescence intensity of mutant TNFSF11 (Fig. 6A). RNA pulldown experiments showed that more hsa-miR-32-3p was enriched in wild-type bio-TNFSF11 (Fig. 6B). Moreover, after overexpression of hsa-miR-32-3p in hBMSCs, the expression level of TNFSF11 mRNA decreased (Fig. 6C).

Effects of hsa-miR-32-3p and TNFSF11 in osteoclasts

After hBMSCs were induced to become osteoclasts, the expression level of hsa-miR-32-3p decreased (Fig. 7A), while the expression level of TNFSF11 mRNA increased (Fig. 7B). After hsa-miR-32-3p mimic was transfected into hBMSCs, TNFSF11 mRNA decreased; but TNFSF11 pcDNA reversed this decrease (Fig. 7C). After hsa-miR-32-3p overexpression, the expression levels of FOS and NFATC1 mRNA in osteoclasts were inhibited; while overexpression of TNFSF11 prevented this effect (Fig. 7D and E). Similarly, the protein levels of cathepsin K and Oscar decreased upon miR-32-3p overexpression, but increased over overexpression of TNFSF11 (Fig. 7F and G). Moreover, transfection of hsa-miR-32-3p mimic reduced the number of osteoclasts; co-overexpression of hsa-miR-32-3p and TNFSF11 had the opposite effect

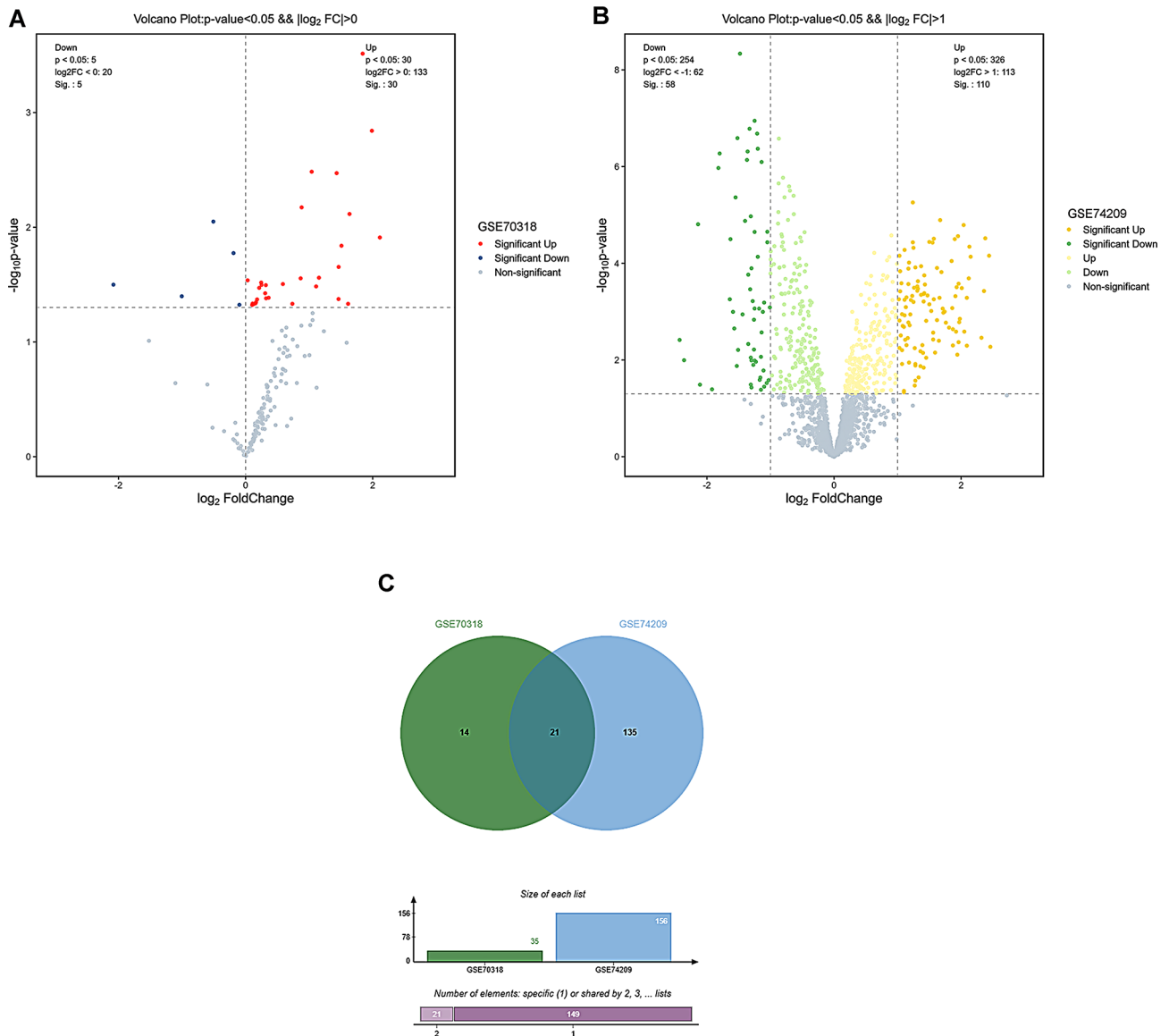


Fig. 2 The differentially expressed miRNAs in osteoporotic fractures. **(A)** Volcano plot for GSE70318 dataset. **(B)** Volcano plot for GSE74209 dataset. **(C)** VENN diagram of differentially expressed miRNAs in GSE70318 and GSE74209 datasets

(Fig. 7H). Therefore, hsa-miR-32-3p may inhibit osteoclast activation via inhibition on TNFSF11 (Fig. 8).

Discussion

In this study, we identified a OF-related miRNA-mRNA axis (miR-32-3p/TNFSF11 axis) using publicly available RNA-seq data. We used the GEO database to search

for osteoporotic fractures, using the GSE70318 and the GSE74209 datasets, and obtained a total of 21 common differentially expressed miRNAs. Through target gene prediction and intersection with OF-related genes, 36 OF-related target genes were obtained. Using the OECloud tools, GO enrichment analysis and KEGG pathway enrichment analysis were performed. We found

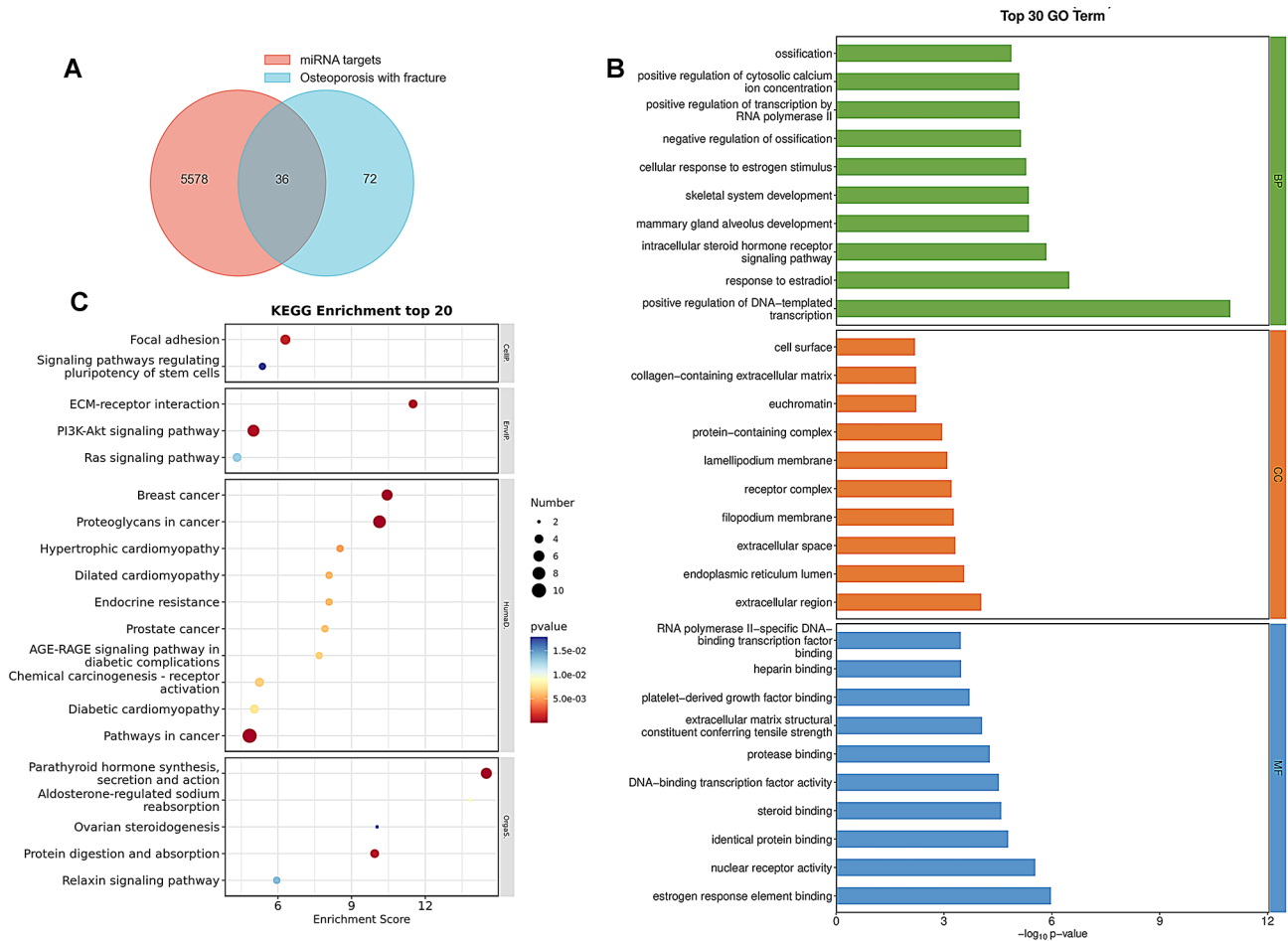


Fig. 3 The potential target genes of differentially expressed miRNAs against osteoporotic fractures. **(A)** VENN diagram of miRNA-target genes and genes related to osteoporotic fracture. **(B)** The top 30 terms of GO enrichment analysis of 36 common genes. **(C)** The top 20 KEGG pathways are enriched by the 36 common genes

that these 36 target genes were enriched in multiple pathways, among which the pathways related to OF included Parathyroid hormone synthesis, secretion, and action. It was found that the axis composed of hsa-miR-32-3p and TNFSF11 can target the OF-related items. Through RT-qPCR analysis, we found that the expression level of hsa-miR-32-3p in low BMD with fractures was lower than that in healthy controls and low BMD without fractures. This was consistent the results from Zhang et al. [27] Zhang et al. reveal that miR-32-3p is lowly expressed was lower in patients with OF than in patients with

osteoporosis, suggesting that miR-32-3p probably is a new diagnosis biomarker for OF [27]. The expression level of TNFSF11 mRNA in low BMD with fractures was higher than that in healthy controls and low BMD without fractures. It can be supposed that hsa-miR-32-3p/TNFSF11 may be involved in the ossification activity of osteoclasts. This study revealed the biological implication of hsa-miR-32-3p/TNFSF11 in OF, suggesting a potential therapeutic target.

Studies have shown that osteoclast recovery is regulated by RANKL signaling [13]. A meta-analysis study

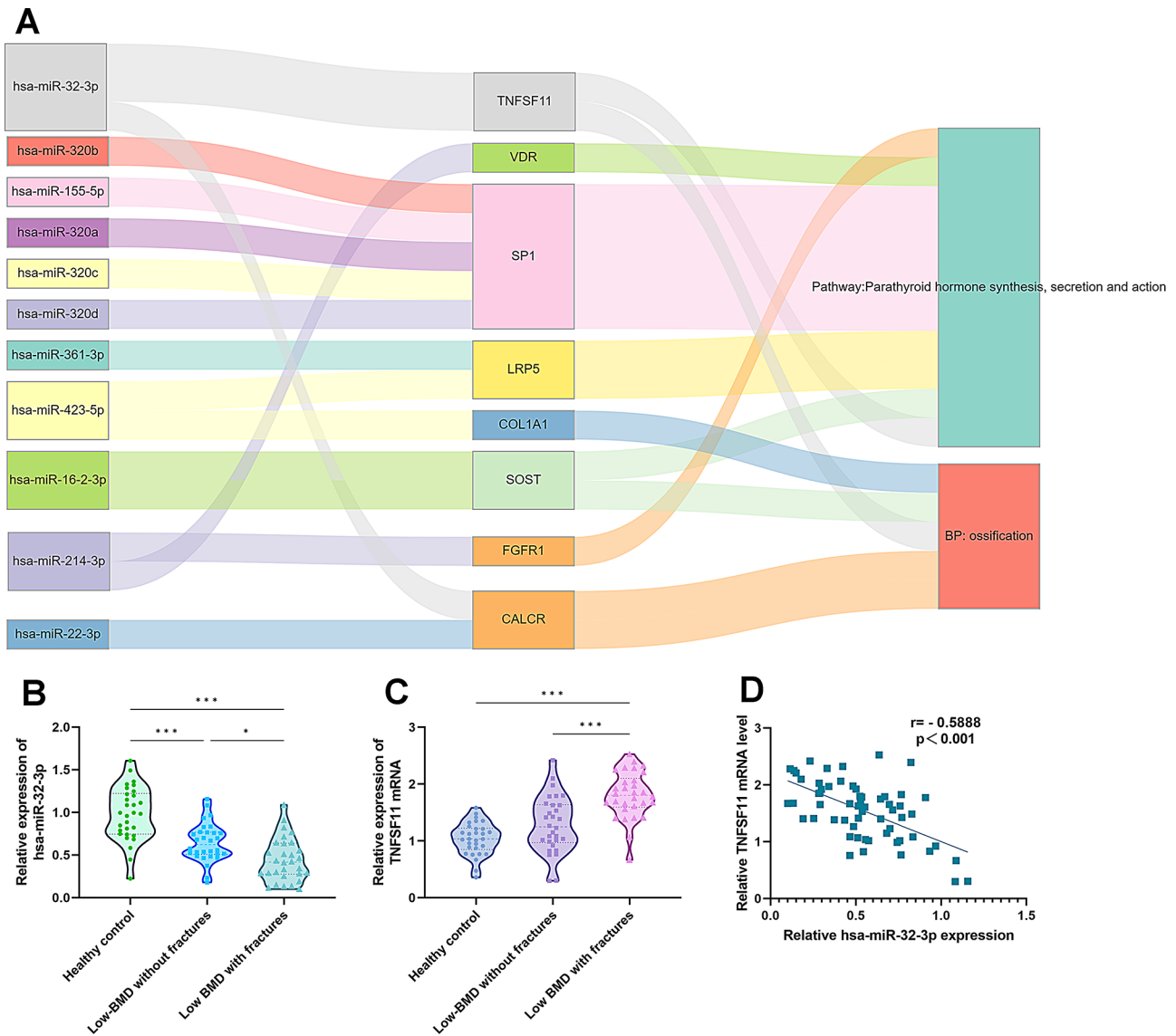


Fig. 5 Hsa-miR-32-3p and TNFSF11 were dysregulated in osteoporotic fracture. **(A)** Sankey plot of miRNA-gene-ossification/Parathyroid hormone synthesis, secretion, and action network. **(B)** Relative expression levels of hsa-miR-32-3p. **(C)** Relative expression level of TNFSF11 mRNA. **(D)** Relationship between the relative expression level of hsa-miR-32-3p and the relative expression level of TNFSF11 mRNA (Pearson analysis)

and TNFSF11, we used hBMSCs to perform dual luciferase reporter experiments and RNA pulldown experiments. Moreover, transfection of hsa-miR-32-3p mimic reduces the number of osteoclasts; co-overexpression of hsa-miR-32-3p and TNFSF11 has the opposite effect. It can be inferred that hsa-miR-32-3p can inhibit the ossification activity of osteoclasts, partly via TNFSF11.

PTH can stimulate the expression of *Tnfsf11* in osteoblasts and osteocytes [31]. Thus, PTH may impact the therapeutic modulation of the miR-32-3p/TNFSF11 axis. Gene dysregulation in human diseases can be influenced by siRNA [32–34]. In this perspective, hsa-miR-32-3p/TNFSF11 axis may be possible therapeutic targets in fracture healing, and may complement or enhance the

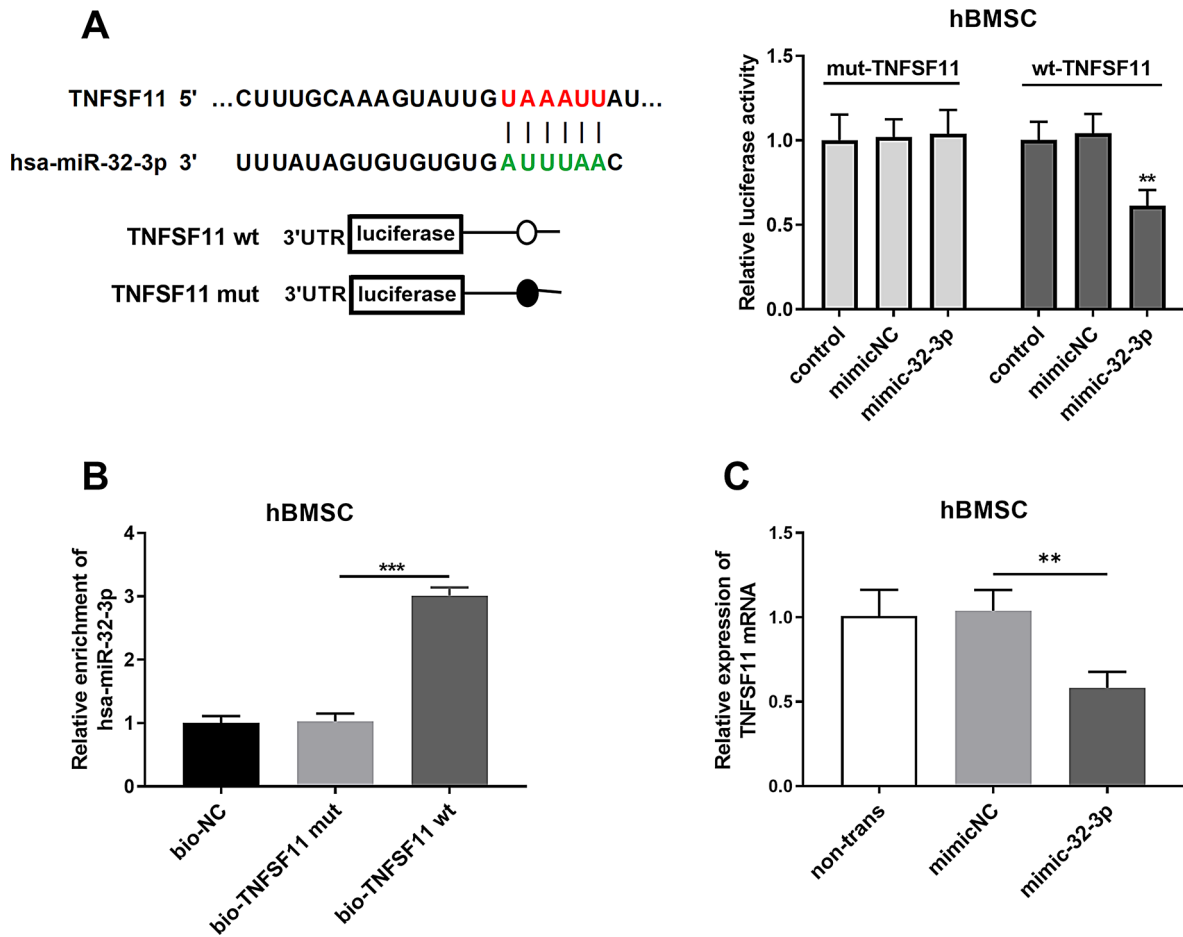


Fig. 6 TNFSF11 was a target of hsa-miR-32-3p. **(A)** Dual luciferase reporter assay. **(B)** RNA pull-down assay. **(C)** Effect of hsa-miR-32-3p mimic on the relative expression level of TNFSF11 mRNA

effects of existing therapies, such as bisphosphonates or teriparatid.

The main drawbacks of our study are as follows: first, lack of in vivo validation, in animals or human. Second, the cases were generated only in a single institution. Thus, it would be interesting to verify the validity by including a population in multi-institution.

To summarize, we constructed miRNA-mRNA networks in OF. These networks proposed the TNFSF11 as a downstream target of hsa-miR-32-3p. Our cell experiments verified that the hsa-miR-32-3p/TNFSF11 axis was involved in the regulation of osteoclast activity. This study proposed hsa-miR-32-3p/TNFSF11 axis as potential therapy targets for OF.

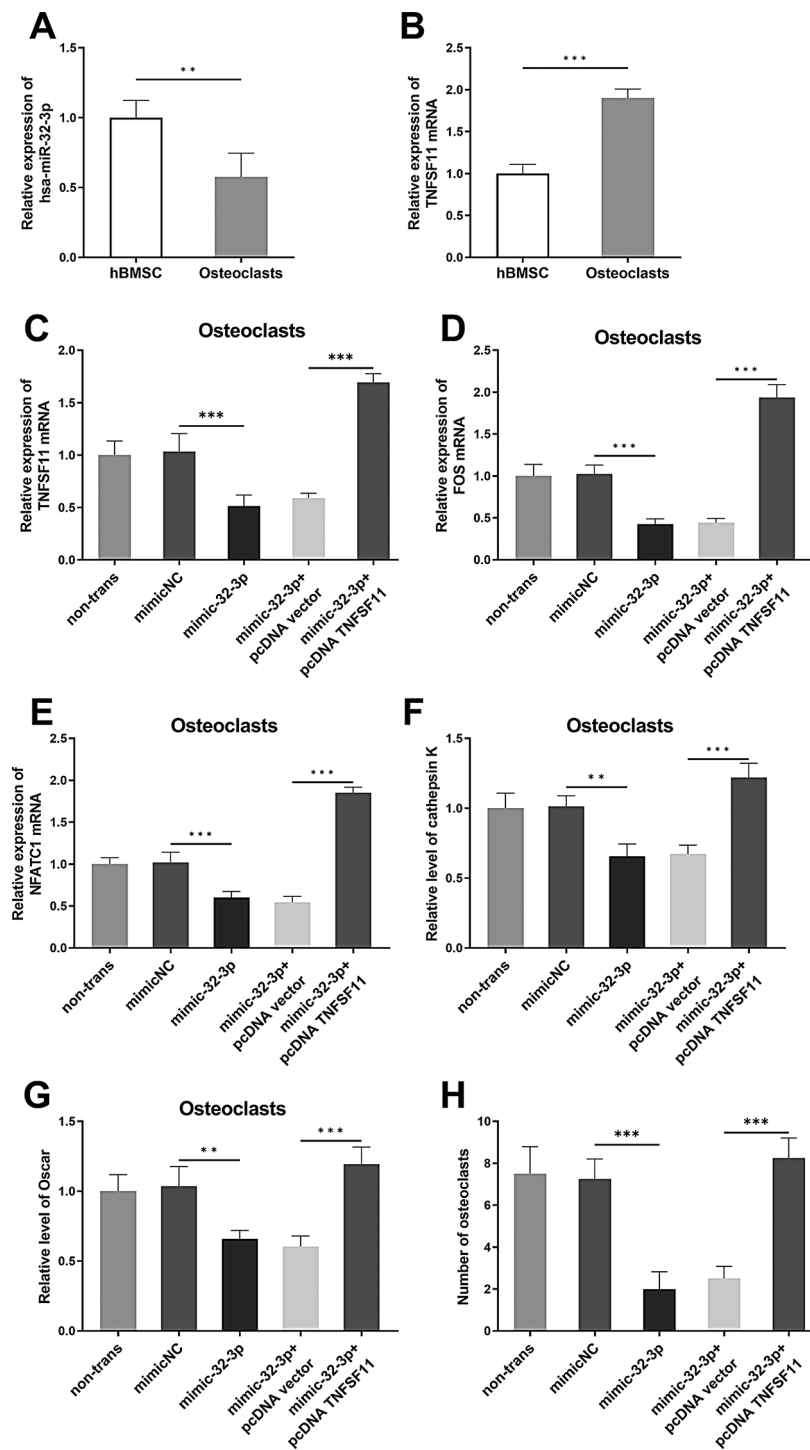


Fig. 7 Hsa-miR-32-3p suppressed osteoclast activity via TNFSF11. **(A)** Changes in the expression level of hsa-miR-32-3p in differentiated osteoclasts. **(B)** Changes in the expression level of TNFSF11 mRNA in differentiated osteoclasts. **(C)** Confirmation of transfection efficiency. **(D)** Expression level of osteoclast marker FOS mRNA. **(E)** Expression level of osteoclast marker NFACT1 mRNA. **(F)** Protein level of osteoclast marker cathepsin K. **(G)** Protein level of osteoclast marker Oscar. **(H)** Number of osteoclasts

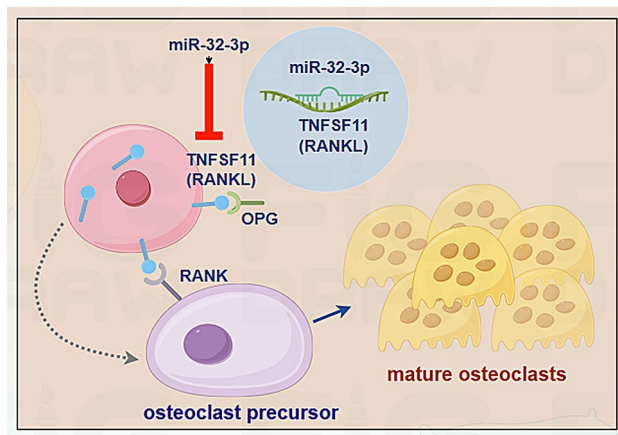


Fig. 8 The potential mechanism of hsa-miR-32-3p/TNFSF11 axis in the regulation of osteoclast activity

Supplementary Information

The online version contains supplementary material available at <https://doi.org/10.1186/s13018-025-05836-7>.

Supplementary Table 1 Baseline data of patients used in the analysis of GSE70318.

Acknowledgements

Not applicable.

Author contributions

Conceptualization, Y.Z., B.Z., J.G., Q.Z., F.Y.; Data curation, Y.Z., B.Z., J.G., Q.Z., F.Y.; Formal analysis, J.G., Q.Z., F.Y.; Funding acquisition, F.Y.; Investigation, J.G., Q.Z.; Methodology, J.G., Q.Z., F.Y.; Project administration, F.Y.; Resources, J.G., Q.Z.; Software, Y.Z., B.Z., J.G., Q.Z.; Supervision, F.Y.; Validation, J.G., Q.Z.; Visualization, J.G., Q.Z.; Roles/Writing - original draft, J.G., Q.Z.; Writing - review & editing, Y.Z., B.Z., F.Y.

Funding

No funding was received to assist with the preparation of this work.

Data availability

The datasets used and/or analysed during the current study are available from the corresponding author on reasonable request.

Declarations

Ethics approval and consent to participate

The study was performed in line with the principles of the Declaration of Helsinki. Approval was granted by the Ethics Committee of Zibo Central Hospital before the study began. The written informed consent has been obtained from the participants involved.

Consent for publication

Not applicable.

Competing interests

The authors declare no competing interests.

Received: 27 February 2025 / Accepted: 22 April 2025

Published online: 29 April 2025

References

- Clynes MA, Harvey NC, Curtis EM, Fuggle NR, Dennison EM, Cooper C. The epidemiology of osteoporosis. *Br Med Bull.* 2020;133(1):105–17.
- Liang B, Burley G, Lin S, Shi YC. Osteoporosis pathogenesis and treatment: existing and emerging avenues. *Cell Mol Biol Lett.* 2022;27(1):72.
- Kim JM, Lin C, Stavre Z, Greenblatt MB, Shim JH. Osteoblast-Osteoclast communication and bone homeostasis. *Cells* 2020; 9(9).
- Kitaura H, Marahleh A, Ohori F, Noguchi T, Shen WR, Qi J et al. Osteocyte-Related cytokines regulate osteoclast formation and bone resorption. *Int J Mol Sci.* 2020; 21(14).
- Qian H, Jia F, Qin H. miR-208a-3p discriminates osteoporosis, predicts fracture, and regulates osteoclast activation through targeting *STC1*. *J Orthop Surg Res.* 2025;20(1):98.
- Migliorini F, Maffulli N, Spiezia F, Peretti GM, Tingart M, Giorgino R. Potential of biomarkers during Pharmacological therapy setting for postmenopausal osteoporosis: a systematic review. *J Orthop Surg Res.* 2021;16(1):351.
- Migliorini F, Maffulli N, Spiezia F, Tingart M, Maria PG, Riccardo G. Biomarkers as therapy monitoring for postmenopausal osteoporosis: a systematic review. *J Orthop Surg Res.* 2021;16(1):318.
- Migliorini F, Colarossi G, Eschweiler J, Oliva F, Driessen A, Maffulli N. Anti-resorptive treatments for corticosteroid-induced osteoporosis: a bayesian network meta-analysis. *Br Med Bull.* 2022;143(1):46–56.
- Conti V, Russomanno G, Corbi G, Toro G, Simeon V, Filippelli W, et al. A polymorphism at the translation start site of the vitamin D receptor gene is associated with the response to anti-osteoporotic therapy in postmenopausal women from Southern Italy. *Int J Mol Sci.* 2015;16(3):5452–66.
- Migliorini F, Giorgino R, Hildebrand F, Spiezia F, Peretti GM, Alessandri-Bonetti M et al. Fragility fractures: risk factors and management in the elderly. *Med (Kaunas).* 2021; 57(10).
- Migliorini F, Maffulli N, Colarossi G, Eschweiler J, Tingart M, Betsch M. Effect of drugs on bone mineral density in postmenopausal osteoporosis: a bayesian network meta-analysis. *J Orthop Surg Res.* 2021;16(1):533.
- Migliorini F, Colarossi G, Baroncini A, Eschweiler J, Tingart M, Maffulli N. Pharmacological management of postmenopausal osteoporosis: a level I evidence Based - Expert opinion. *Expert Rev Clin Pharmacol.* 2021;14(1):105–19.
- Udagawa N, Koide M, Nakamura M, Nakamichi Y, Yamashita T, Uehara S, et al. Osteoclast differentiation by RANKL and OPG signaling pathways. *J Bone Min Metab.* 2021;39(1):19–26.
- Zhu H, Ren J, Wang X, Qin W, Xie Y. Targeting skeletal interocception: a novel mechanistic insight into intervertebral disc degeneration and pain management. *J Orthop Surg Res.* 2025;20(1):159.
- Chi G, Qiu L, Ma J, Wu W, Zhang Y. The association of osteoprotegerin and RANKL with osteoporosis: a systematic review with meta-analysis. *J Orthop Surg Res.* 2023;18(1):839.
- Sun P, Wang M, Yin GY. Endogenous parathyroid hormone (PTH) signals through osteoblasts via RANKL during fracture healing to affect osteoclasts. *Biochem Biophys Res Commun.* 2020;525(4):850–6.
- Yasuda H. Discovery of the RANKL/RANK/OPG system. *J Bone Min Metab.* 2021;39(1):2–11.
- Vishnoi A, Rani S. MiRNA biogenesis and regulation of diseases: an updated overview. *Methods Mol Biol.* 2023;25951:12.
- Diener C, Keller A, Meese E. The miRNA-target interactions: an underestimated intricacy. *Nucleic Acids Res.* 2024;52(4):1544–57.
- Hensley AP, McAlinden A. The role of MicroRNAs in bone development. *Bone.* 2021;143:143115760.
- Giordano L, Porta GD, Peretti GM, Maffulli N. Therapeutic potential of MicroRNA in tendon injuries. *Br Med Bull.* 2020;133(1):79–94.
- Wang S, Liu Z, Wang J, Ji X, Yao Z, Wang X. miR-21 promotes osteoclastogenesis through activation of PI3K/Akt signaling by targeting Pten in RAW264.7 cells. *Mol Med Rep.* 2020;21(3):1125–32.
- Ellur G, Sukhdeo SV, Khan MT, Sharan K. Maternal high protein-diet programs impairment of offspring's bone mass through miR-24-1-5p mediated targeting of SMAD5 in osteoblasts. *Cell Mol Life Sci.* 2021;78(4):1729–44.
- Huang G, Zhao Q, Li W, Jiao J, Zhao X, Feng D, et al. Exosomes: A new option for osteoporosis treatment. *Med (Baltim).* 2022;101(52):e32402.
- Zheng LW, Lan CN, Kong Y, Liu LH, Fan YM, Zhang CJ. Exosomal miR-150 derived from BMSCs inhibits TNF- α -mediated osteoblast apoptosis in osteonecrosis of the femoral head by *GREM1/NF- κ B* signaling. *Regen Med.* 2022;17(10):739–53.
- Kenkre JS, Bassett J. The bone remodelling cycle. *Ann Clin Biochem.* 2018;55(3):308–27.

27. Zhang J, Qian T, Zheng X, Qin H. Role of mir-32-3p in the diagnosis and risk assessment of osteoporotic fractures. *J Orthop Surg Res.* 2024;19(1):709.
28. Almirol EA, Chi LY, Khurana B, Hurwitz S, Bluman EM, Chiodo C, et al. Short-term effects of teriparatide versus placebo on bone biomarkers, structure, and fracture healing in women with lower-extremity stress fractures: A pilot study. *J Clin Transl Endocrinol.* 2016;57(-):14.
29. Eastman K, Gerlach M, Piec I, Greeves J, Fraser W. Effectiveness of parathyroid hormone (PTH) analogues on fracture healing: a meta-analysis. *Osteoporos Int.* 2021;32(8):1531–46.
30. Onal M, St John HC, Danielson AL, Pike JW. Deletion of the distal Tnfsf11 RL-D2 enhancer that contributes to PTH-Mediated RANKL expression in osteoblast lineage cells results in a high bone mass phenotype in mice. *J Bone Min Res.* 2016;31(2):416–29.
31. Zanotti S, Canalis E. Parathyroid hormone inhibits Notch signaling in osteoblasts and osteocytes. *Bone.* 2017;103:159–67.
32. Gargano G, Oliviero A, Oliva F, Maffulli N. Small interfering RNAs in tendon homeostasis. *Br Med Bull.* 2021;138(1):58–67.
33. Gargano G, Oliva F, Oliviero A, Maffulli N. Small interfering RNAs in the management of human rheumatoid arthritis. *Br Med Bull.* 2022;142(1):34–43.
34. Gargano G, Asparago G, Spiezia F, Oliva F, Maffulli N. Small interfering RNAs in the management of human osteoporosis. *Br Med Bull.* 2023;148(1):58–69.

Publisher's note

Springer Nature remains neutral with regard to jurisdictional claims in published maps and institutional affiliations.